

1 **Formate from THF-C1 metabolism induces the AOX1 promoter in formate dehydrogenase-**
2 **deficient *Pichia pastoris***

3

4 Cristina Bustos^{1,2}, Julio Berrios² and Patrick Fickers¹

5

6 ¹ Microbial Processes and Interactions, TERRA Teaching and Research Centre, Gembloux Agro-
7 Bio Tech, University of Liege, Gembloux, Belgium

8 ² School of Biochemical Engineering, Pontificia Universidad Católica de Valparaíso, Av Brasil
9 2085, Valparaiso 2340000, Chile

10

11 Cristina Bustos: cv.bustos@student.Uliege.be, ORCID: 0000-0002-2600-5833

12 Julio Berrios: julio.berrios@pucv.cl, ORCID: 0000-0002-6180-0023

13 Patrick Fickers: pfickers@Uliege.be, ORCID: 0000-0002-2600-5833

14

15

16 **CORRESPONDING AUTHORS:**

17 Patrick Fickers

18 Microbial Processes and Interactions, TERRA Teaching and Research Centre, Gembloux Agro
19 Bio Tech, University of Liege, Gembloux, Belgium

20 pfickers@Uliege.be

21

22 Julio Berrios

23 School of Biochemical Engineering, Pontificia Universidad Católica de Valparaíso, Av Brasil
24 2085, Valparaiso 2340000, Chile

25 julio.berrios@pucv.cl

26

27

28

29 **Abstract**

30 In *Pichia pastoris* (*Komagataella phaffii*), formate is a recognized alternative inducer to
31 methanol for expression systems based on the AOX1 promoter (pAOX1). By disrupting the
32 formate dehydrogenase encoding *FDH1* gene, we converted such a system into a self-induced
33 one, as adding any inducer in the culture medium is no longer requested for pAOX1 induction.
34 In cells, formate is generated from serine through the THF-C1 metabolism, and it cannot be
35 converted into carbon dioxide in an *fdh1Δ* strain. Under non-repressive culture conditions,
36 such as on sorbitol, the intracellular formate generated from the THF-C1 metabolism is
37 sufficient to induce pAOX1 and initiate protein synthesis. This was evidenced for two model
38 proteins, namely intracellular eGFP and secreted CalB lipase from *C. antarctica*. Similar protein
39 productivities were obtained for an *fdh1Δ* strain on sorbitol and a non-disrupted strain on
40 sorbitol-methanol. Considering a *P. pastoris fdh1Δ* strain as a workhorse for recombinant
41 protein synthesis paves the way for the further development of methanol-free processes in *P.*
42 *pastoris*.

43

44

45

46

47

48 Introduction

49 The methylotrophic yeast *Pichia pastoris* (*Komagataella phaffii*) is a well-established and
50 reliable cell factory for producing recombinant proteins (rProt) (Ergün *et al.*, 2021; Barone *et*
51 *al.*, 2023). The expression systems used typically and historically rely on the regulated
52 promoter from the alcohol oxidase 1 gene (pAOX1). This promoter is repressed during cell
53 growth on glycerol, while pAOX1 induction and thus, rProt synthesis, is triggered by adding an
54 inducer to the culture medium, typically methanol (Ergün *et al.*, 2021; Bustos *et al.*, 2022).
55 Although widely used, including on an industrial scale, methanol presents several technical
56 challenges that are difficult to overcome in practice. It is highly flammable and can become
57 toxic to cells at high concentrations due to the accumulation of toxic methanol catabolic
58 products such as formaldehyde (Berrios *et al.*, 2022) (Fig. S1). Moreover, its oxidation by
59 alcohol oxidases in peroxisomes requires oxygen, thereby increasing the cellular oxygen
60 demand compared to other carbon sources. Additionally, methanol catabolism generates
61 heat, which must be dissipated, thereby increasing the operational costs, especially for large-
62 scale production processes (Krainer *et al.*, 2012; Niu *et al.*, 2013).

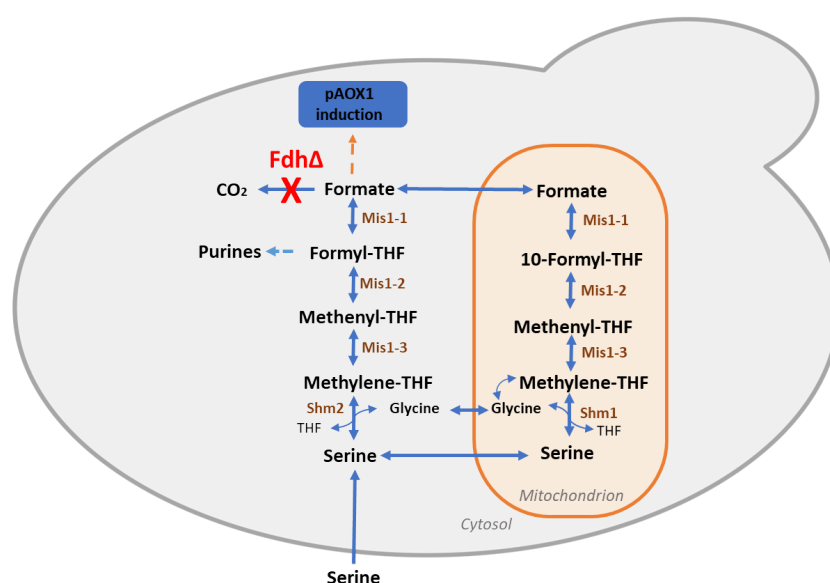
63 Formate, an intermediate metabolite of the methanol dissimilation pathway (Hartner &
64 Glieder, 2006, Fig. S1), has emerged as an interesting alternative inducer to methanol for rProt
65 synthesis in *P. pastoris*. It is produced from formaldehyde by formaldehyde dehydrogenase
66 (Fld) before being converted into carbon dioxide by formate dehydrogenase (Fdh). Compared
67 to methanol, formate is a more sustainable inducer that can be efficiently produced through
68 the electrochemical conversion of carbon dioxide (Jhong *et al.*, 2013; Cotton *et al.*, 2020). The
69 ability of formate to induce pAOX1 has been demonstrated (Tyurin and Kozlov, 2015;
70 Jayachandran *et al.*, 2017; Singh and Narang, 2020). However, one of the primary limitations
71 of formate is its poor ability to be catabolized by *P. pastoris*. To address this constraint, an
72 engineering strategy has been developed through the co-overexpression of genes encoding
73 *Escherichia coli* acetyl-CoA synthase, *Listeria innocua* acetaldehyde dehydrogenase, and the
74 transcription factor Mit1. This engineering effort led to an increase in rProt production (i.e.
75 xylanase, Liu *et al.*, 2022).

76 In cells, formate is also an intermediate of the tetrahydrofolate-mediated one-carbon (THF-C1)
77 metabolism involved in several anabolic pathways, including the *de novo* synthesis of purines
78 (Fig. 1, Kastanos *et al.*, 1997; Piper *et al.*, 2000). It is obtained from cytoplasmic serine by the
79 action of the serine hydroxymethyltransferase (Shm) and the trifunctional C1-tetrahydrofolate
80 synthase (Mis1) (Fig. 1). In the THF-C1 metabolism, formate serves as a shuttle for C1 units
81 between the cytoplasm and the mitochondrion, as THF derivatives cannot cross the
82 mitochondrial membrane (Kastanos *et al.*, 1997).

83 Herein, we aim to investigate the regulation of pAOX1 by formate in an *FDH1* knockout (*fdh1Δ*)
84 strain. From our investigation, it became evident that endogenous formate from THF-C1
85 metabolism was sufficient to trigger pAOX1 induction in an *fdh1Δ* mutant grown under non-
86 repressive culture conditions (i.e. in the presence of sorbitol) without any supplementation of
87 inducer. In those conditions, any pAOX1-based expression system could be potentially
88 converted into a self-induced one.

89
90
91
92
93
94

95



96

97 Figure 1: Tetrahydrofolate (THF) mediated one-carbon (THF-C1) metabolism in yeast. Fdh,
 98 formate dehydrogenase; Shm, serine hydroxymethyltransferase; Mis1, trifunctional C1-
 99 tetrahydrofolate synthase (Mis1-1, Mis1-2, Mis1-3); THF, tetrahydrofolate. FDH gene knockout
 100 is mentioned in red, and enzymes involved in pathways are shown in brown.

101

102 Experimental procedures

103 Strains and media and culture conditions

104 The *P. pastoris* and *Escherichia coli* strains used are listed in Table 1 and S1, respectively. *E. coli*
 105 was cultivated at 37°C in Luria-Bertani medium (LB), supplemented with antibiotics as follows:
 106 100 µg ml⁻¹ ampicillin, 50 µg ml⁻¹ kanamycin, 25 µg ml⁻¹ zeocin, or 50 µg ml⁻¹ hygromycin. *P.*
 107 *pastoris* strains were cultivated at 30°C either in YPD medium (containing 20 g l⁻¹ glucose, 10 g
 108 l⁻¹ Difco yeast extract, and 10 g l⁻¹ Difco bacto peptone) or YNB medium (containing 1.7 g l⁻¹
 109 Difco YNB w/o ammonium chloride and amino acids, 5 g l⁻¹ NH₄Cl and, 0.4 mg l⁻¹ biotin, 100mM
 110 potassium phosphate buffer, pH 6.0) supplemented with as follows: 10 g l⁻¹ sorbitol and 2 g l⁻¹
 111 Difco casamino acid (YNBSC), 10 g l⁻¹ sorbitol, 5.1 g l⁻¹ methanol and 2 g l⁻¹ Difco casamino
 112 acid (YNBSMC); 10 g l⁻¹ sorbitol, 10.8 g l⁻¹ formate and 2 g l⁻¹ Difco casamino acid (YNBSF), 10
 113 g l⁻¹ sorbitol (YNBS), 10 g l⁻¹ sorbitol and 5.1 g l⁻¹ methanol (YNBSM); 10 g l⁻¹ sorbitol and 10.8
 114 g l⁻¹ formate (YNBSF); 10 g l⁻¹ glycerol (YNBG); 6.3 g l⁻¹ methanol and 4.0 g l⁻¹ sorbitol (YNBMS);
 115 10 g l⁻¹ sorbitol and 2 g l⁻¹ serine (YNBSS), 10 g l⁻¹ sorbitol with 2 g l⁻¹ glycine (YNBSG). *P. pastoris*
 116 transformants were selected on YPD agar plates, supplemented with antibiotics as follows
 117 when requested: 25 µg ml⁻¹ zeocin (YPD-Zeo), 200 µg ml⁻¹ hygromycin (YPD-Hygro), 500 µg ml⁻¹
 118 geneticin (YPD-Genet) or 100 µg ml⁻¹ nourseothricin (YPD-Nat).

119 For all cultures, a first preculture inoculated from a single colony was performed for 12 h at
 120 30°C and 150 rpm in a 250 ml shake flask containing 25 ml of liquid YPD medium. After
 121 centrifugation at 9000 g for 5 min, the cells were washed with phosphate-buffered saline (0.1
 122 M, pH 6) before being used to inoculate a second preculture in the same conditions in YNB
 123 media supplemented as described above. Cultures were performed in 24-square deep well
 124 plates (System Duetz, EnzyScreen) as described elsewhere containing 1.5 ml of medium (Sassi
 125 et al. 2016), in 50 ml shake flasks (5 ml medium) or in microbioreactor (BioLector 2, m2p-labs,

126 Baesweiler, Germany). For that purpose, 48-well Flower plates (M2P-MTP-48-B, Beckman
127 Coulter Life Sciences, USA) containing 1 ml of medium were used. Cultures were operated for
128 60h with a relative humidity of 85%, under constant agitation at 1000 rpm. Every 10 minutes,
129 biomass was monitored using scattered light intensity at a wavelength of 620 nm while cell
130 fluorescence was quantified at 520 nm (excitation at 488 nm). The gain was set as 2 for biomass
131 and 4 for fluorescence. Specific fluorescence was obtained by dividing the fluorescence value
132 by the biomass value. It was expressed in specific fluorescence units (sFU). All cultures were
133 seeded at an initial optical density at 600 nm of 0.5 from cells grown in the second preculture.
134 Cultures in 24-square deep well plates were performed with three biological replicates,
135 whereas cultures in the BioLector were performed with two biological replicates, each
136 supported by two technical replicates, resulting in a total of four replicates.
137

Table 1. *Pichia pastoris* strains used in this study.

Name	Parental strain, Genotype	Source/Reference
RIY232	GS115, <i>HIS4</i>	Theron et al (2019)
RIY230	GS115, <i>pAOX1-eGFP</i>	Velastegui et al (2019)
RIY308	GS115, <i>pAOX1-αMF-CalB</i>	Velastegui et al (2019)
RIY536	RIY230, <i>fdh1Δ</i> , <i>pAOX1-eGFP</i> , Zeo+	This work
RIY537	RIY308, <i>fdh1Δ</i> , <i>pAOX1-αMF-CalB</i> , Zeo+	This work
RIY540	RIY536, <i>fdh1Δ</i> , <i>pAOX1-eGFP</i>	This work
RIY561	RIY537, <i>fdh1Δ</i> , <i>pAOX1-αMF-CalB</i>	This work
RIY624	RIY540, <i>fdh1Δ</i> , <i>pAOX1-eGFP</i> , <i>pGAP-FDH1</i> , Zeo+	This work
RIY641	RIY540, <i>fdh1Δ</i> , <i>shm1Δ</i> , <i>pAOX1-eGFP</i> , Nat+	This work
RIY640	RIY540, <i>fdh1Δ</i> , <i>shm2Δ</i> , <i>pAOX1-eGFP</i> , Zeo+	This work
RIY642	RIY540, <i>fdh1Δ</i> , <i>shm1Δ</i> , <i>shm2Δ</i> , <i>pAOX1-eGFP</i> , Zeo+, Nat+	This work

138 *General genetic techniques*

139 Standard media and techniques were used for *E. coli* (Sambrook and Russell, 2001). Restriction
140 enzymes, DNA polymerases, and T4 DNA ligase were obtained from New England Biolabs (NEB,
141 Ipswich, MA, USA) or Thermo Scientific (Thermo Scientific, Waltham, MA USA). Primers for
142 PCR and qPCR were synthesized by Eurogentec (Seraing, Belgium, Table S2). Vector TopoBluntII
143 and pGEMTeasy were from Invitrogen (Waltham, Massachusetts, United States) and Promega
144 (Madison, Wisconsin, United States), respectively. Genomic DNA was purified using a Genomic
145 DNA Purification kit (Thermo Scientific, Waltham, MA USA). DNA fragments were purified from
146 agarose gels using a NucleoSpin Gel and a PCR clean-up kit (Machery-Nagel, Düren, Germany).
147 DNA sequencing was performed by Eurofin Genomic (Eurofin, Ebersberg, Germany).
148 Quantitative PCR (qPCR) were performed as described elsewhere with primers listed in Table
149 S1, using the actin gene as a reference. Total RNA was extracted using the NucleoSpin RNA Plus
150 kit (Machery-Nagel, Düren, Germany). qPCR was performed using the Luna Universal qPCR
151 Master Mix and the Step OnePlus Real-Time PCR system (Thermo Scientific, Waltham, MA,
152 USA). Primers and plasmid designs were performed using the software Snapgene (Dotmatics,
153 USA). Vectors were constructed using the GoldenPiCS Kit (Prielhofer et al., 2017, Addgene kit
154 #1000000133). *P. pastoris* was transformed as described by Lin-Cereghino et al., (2005).
155

156 *Construction of plasmids and P. pastoris strains*

157 To construct the gene disruption cassettes, a ~ 1kb fragment upstream of the start codon (Pro-
158 gene) and ~ 1kb fragment downstream of the stop codon (Term-gene) of the genes

159 PAS_chr3_0932 (*FDH1*), PAS_chr4_0587 (*SHM1*) and PAS_chr4_0415 (*SHM2*) were PCR-
160 amplified using *P. pastoris* GS115 genomic DNA as a template. The primer pairs used to amplify
161 Pro-gene and Term-gene were P.fdh1-Fw/P.fdh1-Rv and T.fdh1-Fw/T.fdh1-Rv for *FDH1*, P.shm1-
162 Fw/P.shm1-Rv and T.smh1-Fw/T.shm1-Rv for *SHM1*; and P.shm2-Fw/P.shm2-Rv and T.smh2-
163 Fw/T.shm2-Rv for *SHM2*. The zeocin and nourseothricin selection markers were amplified from
164 plasmids D12-BB3aZ_14 and E6-BB3aN_14 (Table S1), used as a template with primer pairs
165 BleoR.fdh1-Fw/BleoR.fdh1-Rv, Nat.shm1-Fw/Nat.shm1-Rv and BleoR.shm2-Fw/ BleoR.shm2-
166 Rv and subsequently used to construct the *FDH1*, *SHM1* and *SHM2* disruption cassettes,
167 respectively. The *FDH1* disruption cassette (P_fdh1-Bleo.R-T_fdh1) was obtained by Golden
168 Gate assembly using BsaI as restriction enzyme. The *SHM1* and *SHM2* disruption cassettes
169 (Pro_gene-Selection Marker-Term_gene) were obtained by an overlapping PCR using the
170 corresponding purified Pro_gene, selection marker, Term_gene fragment as templates and
171 primer pairs P.fdh1-Fw/T.fdh1-Rv, P.shm1-Fw/T.shm1-Rv and P.shm2-Fw/T.shm2-Rv,
172 respectively. The resulting ~ 3.2 kb fragments were cloned into the pGEMT-Easy vector or Blunt
173 II-Topo vector to generate plasmids RIP 369 (*FDH*), RIP491 (*SHM2*), RIP492 (*SHM1*) (Table S1).
174 The *FDH1* disruption cassette from plasmid RIP369 was subsequently used to transform strains
175 RIY230 (pAOX1-eGFP) and RIY308 (pAOX1- α MF-CalB) to yield strains RIY536 (*fdh* Δ , pAOX1-
176 eGFP, Zeo+) and RIY537 (*fdh* Δ , pAOX1- α MF-CalB, Zeo+), respectively. Construction of strains
177 RIY230 and RIY308 were described in Velastegui et al., (2019). The *SMH1* and *SHM2* disruption
178 cassettes from plasmids RIP492 and RIP491 were used to transform strain RIY540 to generate
179 the strains RIY639, RIY641 and RIY642 (Table 1). The disruption cassettes were released from
180 the corresponding plasmid by SacI restriction. Transformants were selected on YPD-Zeo and
181 YPD-Nat, according to the corresponding marker. For marker rescue, strains RIY536, and
182 RIY237 were transformed with the replicative vector RIP396 (pKTAC-Cre) and transformants
183 were selected YPD-Genet. The resulting strains were RIY540 (*fdh* Δ , pAOX1-eGFP) and RIY561
184 (*fdh* Δ , pAOX1- α MF-CalB). To construct the *FDH1* expression vector, the GoldenPiCS system was
185 used (Prielhofer et al., 2017). Internal Bpil recognition sequence in gene PAS_chr3_0932
186 (*FDH1*) was removed by overlapping PCR using pairs Fdh1-Fw/Fdh1.Bpil-Rv and Fdh1.Bpil-
187 Fw/Fdh1-Rv using *P. pastoris* GS115 genomic DNA as a template. The resulting PCR product
188 was cloned into plasmid A2 (BB1-23) at BsaI restriction site to yield plasmid RIP465. Plasmid
189 RIP466 (pGAP-FDH1-ScCYC1tt) was constructed by Golden Gate assembly from the plasmids
190 RIP465, A4 (BB1_12_pGAP), C1 (BB1_34_ScCYC1tt) and E1. (BB3eH_14) using Bpil as the
191 restriction enzyme. After PmeI digestion and purification, plasmid RIP466 was used to
192 transform the RIY540 strain (*fdh* Δ , pAOX1-eGFP) to yield the RIY624 strain (pAOX1-EGFP, pGAP-
193 FDH). Transformants were selected on YPD-Hygro. Correctness of the disruption mutant
194 genotype was confirmed by analytical PCR on the genomic DNA of the different disrupted
195 strains. For gene disruption, the forward primers annealed upstream of the Pro-genes, namely
196 Up.fdh1-Fw, Up.shm1-Fw, Up.shm2-Fw, for genes *FDH1*, *SHM1* and *SHM2*, respectively, while
197 the reverse primers annealed within the selection marker, namely BleoR.Int-Rv for genes *FDH1*
198 and *SHM2*, and Nat.shm1-Rv for gene *SHM1*. As further confirmation, forward primers that
199 annealed within the selection marker BleoR.Int-Fw for gene *FDH1* and *SHM2*, and Nat.Int-Fw
200 for gene *SHM1* and reverse primers that annealed downstream of the Term-gene, namely Dw.
201 fdh1-Rv, Dw.shm1-Rv, Dw.shm2-Rv, for gene *FDH1*, *SHM1* and *SHM2*, respectively, were used.
202 To confirm the excision of the selection marker in the *fdh1* Δ strain RIY536, primer pairs P.fdh1-
203 Fw/T.fdh1-Rv were used. To verify the genotype of the RIY624 strain (*FDH1* complemented
204 strain), primers pGAp.Int-Fw and Cyc1t.Int-Rv that annealed in the pGAP and the ScCYC1tt
205 region were used.

206 *Analytical methods.*

207 Cell growth was monitored either by optical density at 600nm (OD₆₀₀) or dry cell weight (DCW)
208 as previously described (Carly *et al.*, 2016). Methanol, sorbitol, and glycerol concentrations
209 were determined by HPLC (Agilent 1100 series equipped-RID detector, Agilent Technologies,
210 Santa Clara, CA, USA) using an Aminex HPX-87H ion-exclusion column (300 × 7.8 mm Bio-Rad,
211 Hercules, CA, USA). Compounds were eluted from the column at 65 °C with a flow rate of 0.5
212 ml min⁻¹ and using a 5 mM H₂SO₄ solution as the mobile phase.

213 Intracellular eGFP fluorescence was quantified using a BD Accuri C6 Flow Cytometer (BD
214 Biosciences, San Jose, CA, USA) as described elsewhere (Sassi *et al.*, 2016). For each sample,
215 20,000 cells were analyzed using the FL1-A and FSC channels, and FL1-A/FSC dot plots were
216 analyzed using the CFlowPlus software (Accuri, BD Biosciences). A threshold of 5800
217 fluorescence units (FU) on FL1-A channel was applied to eliminate the noise for endogenous
218 fluorescence from the cells. To calculate the total value of fluorescence in the cell population,
219 the FL1-A median value (i.e., the eGFP fluorescence) was multiplied by the fraction of cells
220 with eGFP fluorescence (i.e., induced cells). It was expressed in total fluorescence unit (TFU).
221 Spectrophotometric analysis of eGFP was performed on SpectraMax M2 (Molecular Devices,
222 San Jose San Jose, CA, USA) using λ_{ex} and λ_{em} at 488 and 535 nm, respectively. Measurements
223 were taken after 30 s of sample shaking. Signal gain was set to 225, and the number of light
224 flashes was set to 30. Specific eGFP fluorescence was expressed as specific fluorescence units
225 (SFU), i.e., as fluorescence value normalized to biomass related to optical density at 600 nm
226 (OD₆₀₀) of 0.5.

227 The lipase activity in the culture supernatant was determined by monitoring the hydrolysis of
228 p-nitrophenylbutyrate (p-NPB) as described elsewhere (Fickers *et al.*, 2003). The release of
229 para-nitrophenol was monitored at 405 nm using a SpectraMax M2 (Molecular Devices, San
230 Jose, CA, USA). All lipase activity assays were performed at least in triplicate. One unit of lipase
231 activity was defined as the amount of enzyme releasing 1 μ mol p-nitrophenol per minute at
232 25 °C and pH 7.2 (ϵ PNP = 0.0148 μ M⁻¹.cm⁻¹).

233

234 *Fluorescence microscopy*

235 Microscopy was performed with a Nikon Eclipse Ti2-E inverted automated epifluorescence
236 microscope (Nikon Eclipse Ti2-E, Nikon France, France) equipped with a DS-Qi2 camera (Nikon
237 camera DSQi2, Nikon France, France), a 100× oil objective (CFI P-Apo DM Lambda 100× Oil
238 (Ph3), Nikon France, France). The GFP-3035D cube (excitation filter: 472/30 nm, dichroic
239 mirror: 495 nm, emission filter: 520/35 nm, Nikon France, Nikon) was used to visualize eGFP.
240 Prior observation, cells were washed with phosphate buffer saline and diluted at a cell
241 concentration of 0.5 gDCW l⁻¹. For image processing, ImageJ software was used (Collins, 2007;
242 Schneider *et al.*, 2012).

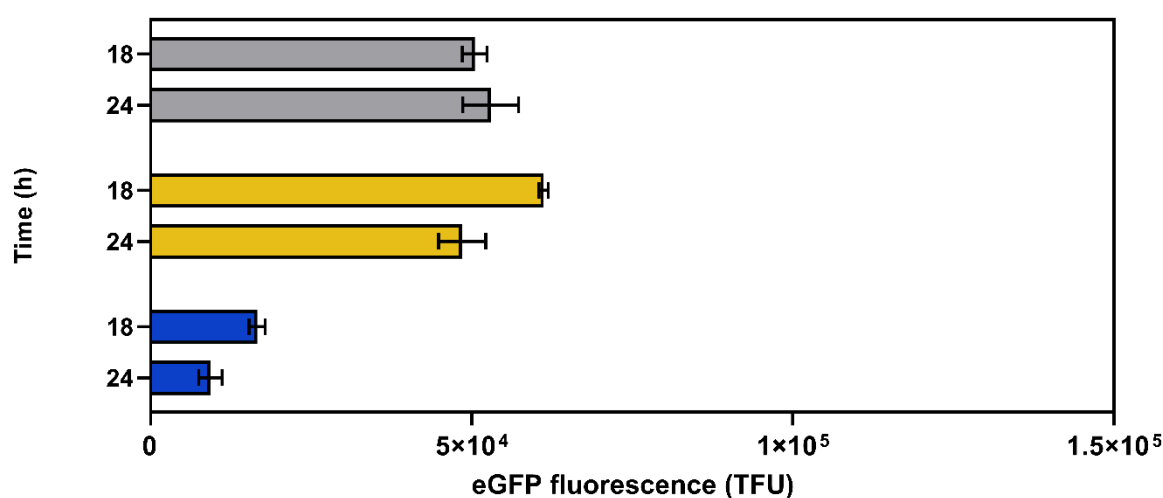
243

244 **Results and discussion**

245 ***AOX1 promoter activity is upregulated by formate***

246 In methylotrophic yeasts, formate is an intermediate of the methanol dissimilation pathway
247 (Hartner & Glieder, 2006, Fig. S1). Studies have demonstrated the efficacy of formate as both
248 an inducer and a carbon source to produce recombinant proteins (rProt) in *P. pastoris* (Singh
249 and Narang, 2020; Liu, Li, *et al.*, 2022; Liu, Zhao, *et al.*, 2022). Herein, an enhanced green
250 fluorescent protein (eGFP) reporter system was used to probe the regulation of the *AOX1* gene
251 promoter (*pAOX1*) by formate. For this purpose, the RIY230 strain (*pAOX1-eGFP*, hereafter
252 *FDH1* strain, (Velastegui *et al.*, 2019) was grown on sorbitol (YNBS) supplemented or not with

253 methanol or formate (YNBSC, YNBSCM, and YNBSCF, respectively). Sorbitol was selected as
254 the carbon source since it is known as non-repressive for pAOX1 (Niu *et al.*, 2013). Specific
255 eGFP fluorescence was monitored in cells by flow cytometry at the end of the growth phase
256 (i.e., 18h) and during the stationary phase (i.e., 24h). As shown in Fig. 2, the pAOX1 induction
257 levels (eGFP signal) were low on sorbitol medium (16601 and 9340 TFU, respectively). They
258 were remarkably higher and in the same range for cells grown on sorbitol-methanol (61207
259 and 48518 TFU, respectively) or sorbitol-formate (50488 and 52960 TFU, respectively). These
260 observations contrast with a recent report on similar experiments conducted on glycerol-
261 based defined media (YNBG), where eGFP-specific fluorescence levels were reported as 4.1-
262 fold lower in the presence of formate compared to methanol (Feng *et al.*, 2022). This
263 demonstrates that formate can substitute methanol for pAOX1 induction, at least in a sorbitol-
264 minimal medium.
265



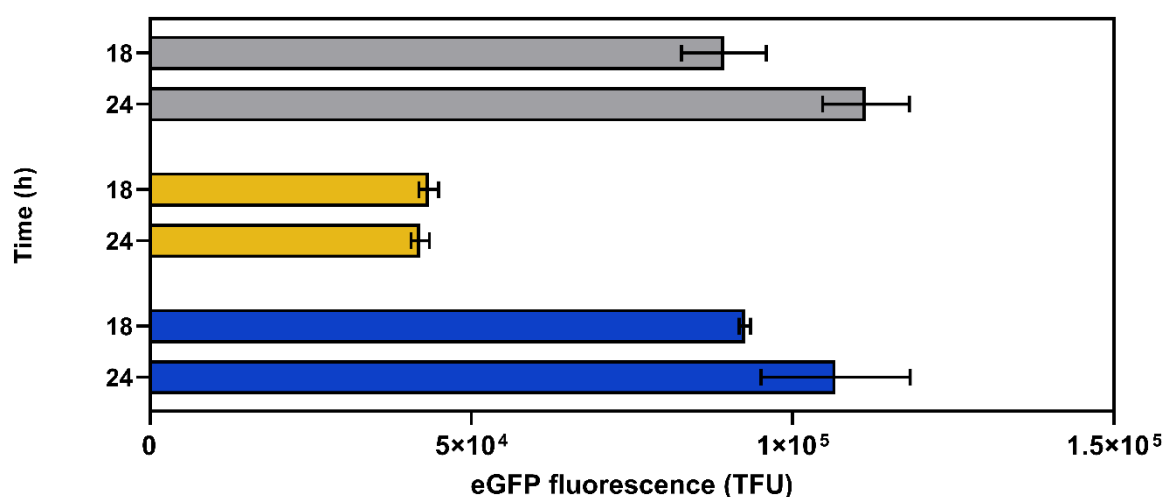
266

267 Figure 2: eGFP fluorescence of RIY230 strain (pAOX1-eGFP, FDH1 strain) after 18h and 24 h of growth
268 in YNB minimal medium containing sorbitol and formate (YNBSCF, grey), sorbitol and methanol
269 (YNBSCM, yellow), and sorbitol (YNBSC, blue). Fluorescence was quantified by flow cytometry on
270 20,000 cells and expressed as TFU (total fluorescence, see materials and method for calculation
271 details). Data are the mean and standard deviation of triplicate cultures conducted in deep well plates.
272

273 **Formate can be used as a free inducer in an *fdh1Δ* strain**

274 In the methanol dissimilation pathway, formate is converted to carbon dioxide by formate
275 dehydrogenase (Fdh, Fig. S1). In methylotrophic yeasts, including *P. pastoris*, Fdh was shown
276 as non-essential for cell survival. However, the growth of a formate dehydrogenase knockout
277 mutant (*fdh1Δ*) is remarkably reduced in a methanol-based medium (Guo *et al.*, 2021).
278 Moreover, an *fdh1Δ* strain exhibits a heightened sensitivity to the accumulation of formate in
279 the medium, indicating that the primary physiological function of Fdh is more related to the
280 detoxification of intracellular formate rather than energy generation (Sibirny *et al.*, 1990; Sakai
281 *et al.*, 1998). Therefore, the knockout of gene *FDH1* in *P. pastoris* would render formate a free
282 pAOX1 inducer in non-repressive conditions (in the presence of sorbitol). For that purpose, the
283 *FDH1* knockout RIY540 strain (*fdh1Δ*, pAOX1-eGFP, hereafter *fdh1Δ*, Table 1) was constructed.
284 It was grown on sorbitol, sorbitol-methanol, or sorbitol-formate (YNBSC, YNBSCM, and
285 YNBSCF, respectively), and the eGFP fluorescence was quantified by flow cytometry after 18 h
286 and 24 h of culture. On sorbitol-methanol (YNBMC), eGFP fluorescence signals were on

287 average for both sampling times in the same range for the *fdh1Δ* and *FDH1* strains (i.e. 42715
288 and 54862 TFU, respectively; Fig. 2 and 3). This demonstrates that the knockout of *FDH1* has
289 no impact on the strength of the pAOX1 induction level by methanol. By contrast, on sorbitol-
290 formate, the fluorescence signals were, on average, for both sampling times 1.9-fold higher
291 for the *fdh1Δ* strain compared to the *FDH1* strain (i.e. 100359 and 51724 TFU, respectively).
292 Therefore, preventing *P. pastoris* from dissipating formate into carbon dioxide yielded higher
293 induction levels of pAOX1 on formate than on methanol. More importantly, for the *FDH1*-
294 knockout strain, eGFP fluorescence signals were in the same range on sorbitol and sorbitol-
295 formate on average for the two sampling times (i.e. 99632 and 100359 TFU, respectively). It
296 was also 7.6-fold higher on average for the *fdh1Δ* strain compared to the *FDH1* strain on
297 sorbitol (i.e., in the absence of any inducer; 99632 and 12970 TFU). These results were
298 corroborated by quantifying the eGFP gene expression level for the *fdh1Δ* strain grown on
299 sorbitol. It was 2.9 and 3.2-fold increased the *fdh1Δ* strain compared to the *FDH1* strain after
300 18 h and 24 h of growth, respectively (Fig. S2). Fluorescence microscopy also clearly showed a
301 higher eGFP level for the knockout strain on sorbitol (i.e. without the addition of formate; Fig.
302 S3).



303

304 Figure 3. eGFP fluorescence of RY540 strain (*fdhΔ*, pAOX1-eGFP, *fdh1Δ* strain) after 18h and 24 h of
305 growth in YNB minimal medium containing sorbitol and formate (YNBSFC, grey), sorbitol and methanol
306 (YNBSMC, yellow), and sorbitol (YNBSC, blue). Fluorescence was quantified by flow cytometry on
307 20,000 cells and expressed as TFU (total fluorescence, see materials and method for calculation
308 details). Data are the mean and standard deviation of triplicate cultures conducted in deepwell plates.
309

310 **Complementation of the *fdh1Δ* strain restored the wild-type phenotype**

311 To confirm that the phenotype of the *fdh1Δ* strain is related to the disruption of the gene
312 PAS_chr3_0932, it was expressed under the control of the constitutive pGAP promoter in the
313 RY540 strain. The resulting RY624 strain (*fdh1Δ*, pAOX1-eGFP, pGAP-FDH, hereafter *fdh1Δ*-
314 *FDH1*) was grown on sorbitol (YNBS) together with *FDH1* and *fdh1Δ* strains, used as negative
315 and positive controls, respectively. The fluorescence level of the *fdh1Δ*-*FDH1* strain was
316 reduced by 24-fold on average on two sampling times (18 h and 24 h) as compared to the
317 *fdh1Δ* strain (i.e. 87218 and 3657 TFU, respectively; Fig. S4). This demonstrates that the
318 disruption of the *FDH1* gene is related to the phenotype of the knockout strain.
319

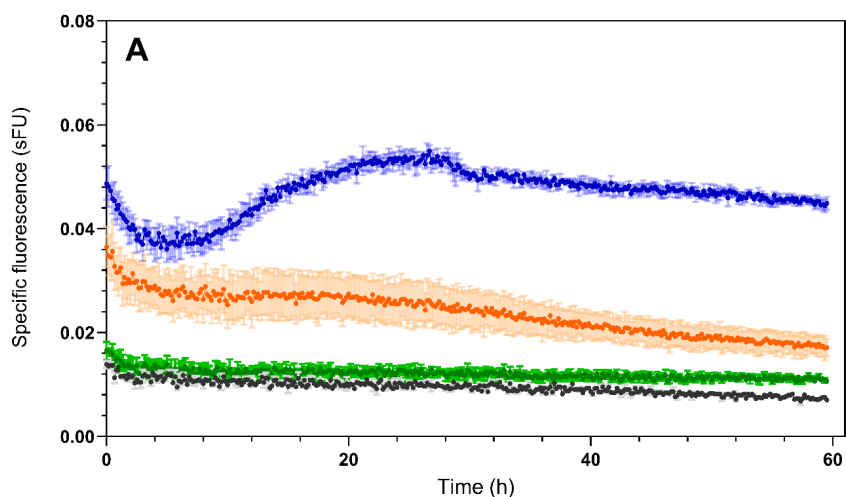
319

320

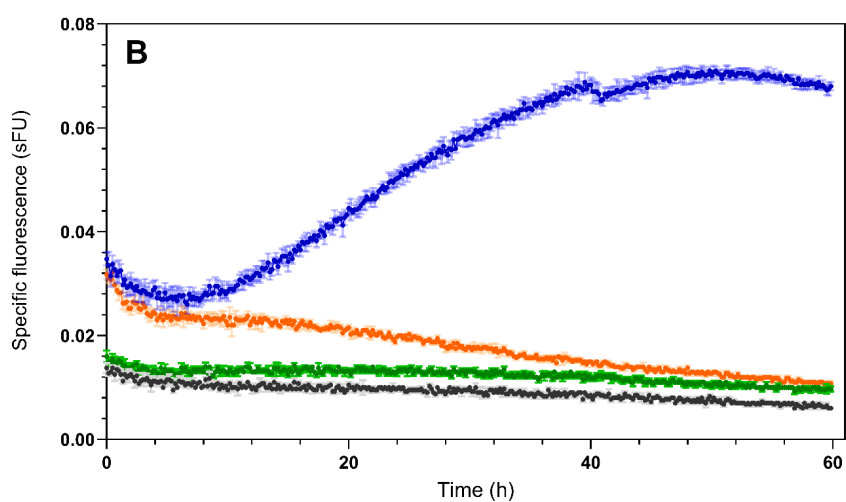
321 **Unravelling the origins of formate in a methanol-free environment**

322 In the *fdh1Δ* strain, a strong increase in the pAOX1 induction level was observed under non-
323 repressive culture conditions and in the absence of formate compared to the FDH1 strain (on
324 sorbitol medium, YNBSC). This suggests that formate is generated in an alternative metabolic
325 pathway and somehow accumulates intracellularly in the *fdh1Δ* strain. Besides the methanol
326 dissimilation pathway, formate is generated from cytoplasmic serine in the THF-C1 metabolism
327 by Shm1 and Mis1 enzymes (Fig. 1, Kastanos et al., 1997). In a *P. pastoris* wild-type strain,
328 formate generated through that metabolism can, therefore, be consumed either by Mis1 to
329 form formyl-THF or by Fdh to form carbon dioxide. As the disruption of gene *FDH1* prevent this
330 conversion into carbon dioxide, formate may somehow accumulate intracellularly in the *fdh1Δ*
331 strain, explaining thus the induction level of pAOX1 in non-repressive conditions. To verify this
332 hypothesis, the expression of gene *FDH1* (as well as *FGH1* and *FLD*) was first confirmed by qPCR
333 in cells grown on sorbitol (YNBS, Fig. S5). We then try to increase the intracellular formate
334 formation through the THF-C1 pathway indirectly by the addition of serine in the culture
335 medium. Therefore, *FDH1* and *fdh1Δ* strains were grown in sorbitol-based media
336 supplemented or not with serine (YNBS and YNBSS, respectively), and the specific fluorescence
337 (i.e. normalized to biomass) was monitored over 60 h. For the *FDH1* strain, the fluorescence
338 signal remained at a constant and low level, similar to the RIY232 strain (GS115 prototroph),
339 on both media and throughout the entire cultivation period (Fig. 4A & B). This suggests that
340 pAOX1 is most probably not induced in those conditions in the *FDH1* strain. By contrast, the
341 fluorescence signal and thus pAOX1 induction level were remarkably higher for the *fdh1Δ*
342 strain, especially on a medium supplemented with serine. The specific fluorescence values for
343 the *fdh1Δ* strain after 60 h of growth were 4.0 and 6.1-fold increased on sorbitol and sorbitol-
344 serine, respectively, compared to the *FDH1* strain. Moreover, the addition of serine in the
345 medium yielded for the *fdh1Δ* strain a 1.5-fold increased fluorescence signal compared to the
346 non-supplemented medium. Similarly, we tried to decrease the intracellular formate
347 formation through the THF-C1 pathway by growing the cell in the presence of glycine, as it has
348 been reported as a Shm inhibitor (Piper et al., 2000). As shown in Fig 4C, the addition of glycine
349 impaired pAOX1 induction for both strains for over 50 h. Gene PAS_chr4_0415 (*SHM2*)
350 encoding cytoplasmic Shm was also disrupted in the *fdh1Δ* strain. The resulting RIY640 strain
351 (*fdh1Δ, shm2Δ, pAOX1-eGFP*, hereafter *fdh1Δ-shm2Δ*) was grown on sorbitol in the presence
352 or not of serine or glycine (YNBS, YNBSS and YNBSSG, respectively). In all tested media, the
353 specific fluorescence signal was markedly lower for *fdh1Δ-shm2Δ* strain as compared to the
354 *fdh1Δ* strain (Fig. 4). By contrast, disruption of genes PAS_chr4_0587 (*SHM1*) encoding
355 mitochondrial (Shm1) did not reduce remarkably the eGFP fluorescence (Fig S6). These
356 findings substantiate the hypothesis that the intracellular formate is higher in the *fdh1Δ* strain,
357 accounting for pAOX1 induction in non-repressive culture conditions.

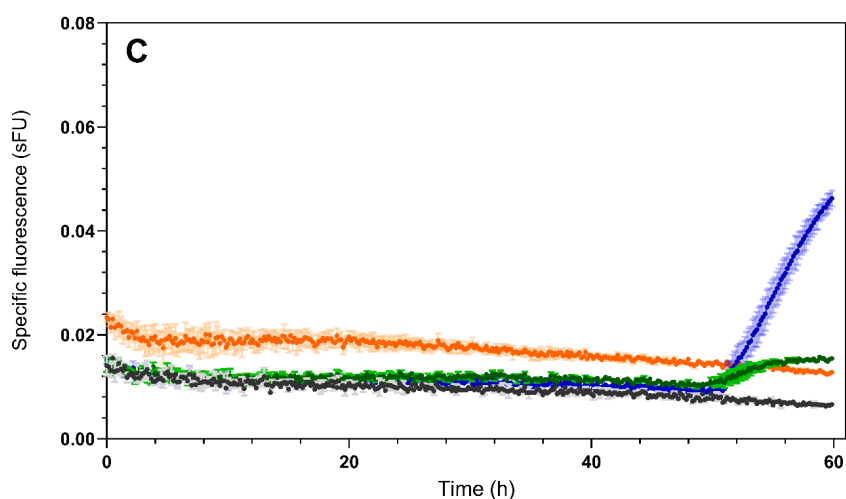
358
359



360



361



362

363 Figure 4: Specific eGFP fluorescence of RIY232 (WT, black); RIY230 (pAOX1-eGFP, green);
364 RIY540 (fdhΔ, pAOX1-EGFP; blue); RIY640 (fdhΔ, shm2Δ pAOX1-eGFP; orange) strains;
365 during growth in YNB minimal medium containing sorbitol (YNBS, panel A), sorbitol and serine
366 (YNBSS, panel B), and sorbitol and glycine (YNBSSG, panel C) Cells were grown in BioLector and

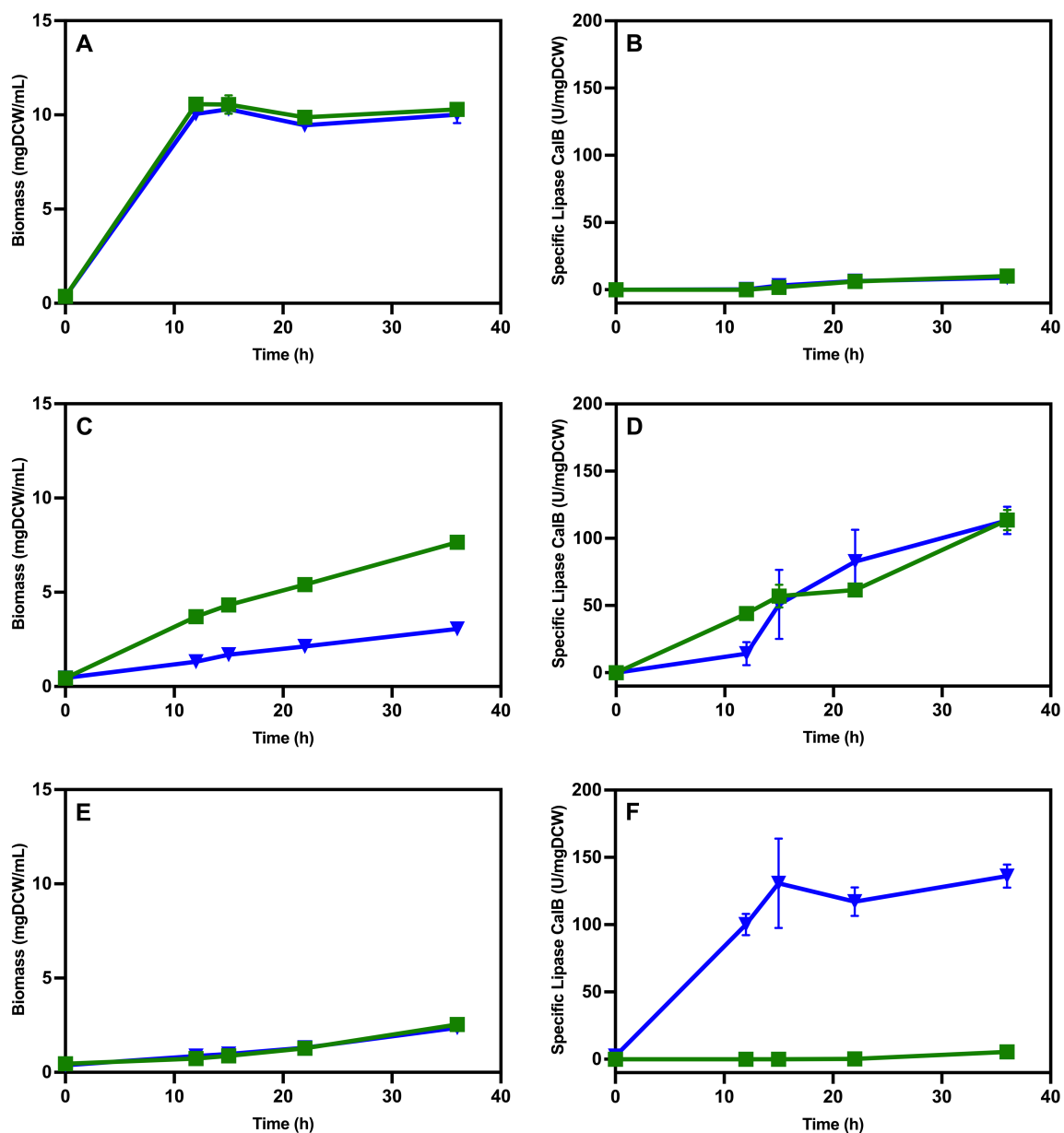
367 specific fluorescence values are means and standard deviation on four cultures replicates. sFU:
368 specific fluorescence unit.

369

370 **Production of a secreted protein by an *fdh1Δ* mutant in sorbitol-based medium**

371 In many recombinant protein (rProt) production processes using *P. pastoris*, glycerol is used in
372 a first phase to generate biomass at a high cell density, to repress pAOX1 and thus to prevent
373 rProt synthesis. In a second phase, the carbon source is shifted to methanol or to a mixture of
374 methanol and sorbitol to trigger rProt synthesis by induction of pAOX1 promoter (Niu *et al.*,
375 2013; Carly *et al.*, 2016; Berrios *et al.*, 2017). In the rProt production phase, the purpose is to
376 direct most of the energy from carbon sources to rProt synthesis while minimizing cell growth.
377 Herein, the lipase B from *Candida antarctica* (CalB) was used in combination with the α -mating
378 factor from *S. cerevisiae* as a secretory protein reporter. The CalB coding sequence was cloned
379 under the control of the pAOX1 promoter and integrated into the genome of the RIY232 strain,
380 a prototroph derivative of *P. pastoris* GS115 (Velastegui *et al.*, 2019). In the resulting RIY308
381 strain (*pAOX1- α MF-CalB*, CalB strain), the *FDH1* encoding gene was then knockout to yield the
382 RIY561 strain (*fdh1Δ*, *pAOX1- α MF-CalB*, CalB-*fdh1Δ* strain). Both strains were grown either on
383 glycerol, on a mixture of methanol and sorbitol (60/40, 0.3 C-mol as in Carly *et al.*, 2016; Niu
384 *et al.*, 2013), and on sorbitol (i.e., YNBG, YNBMS and YNBS, respectively). Biomass and specific
385 lipase CalB activity were quantified at different time points over 36 h (Fig.5).

386 On glycerol, cell growth for the CalB and the CalB-*fdh1Δ* strains were similar, with biomass
387 values equal to 10.6 ± 0.1 and 10.1 ± 0.3 gDCW l⁻¹, respectively, at the end of the growth phase
388 (i.e., 12h, Fig 5.A). As expected, the lipase activity could not be detected during the first 12h,
389 then after it increased slightly upon glycerol exhaustion in the medium (i.e. in pAOX1
390 derepressed condition, data not shown). On methanol (YNBSM), the biomass of the CalB-
391 *fdh1Δ* strain was markedly lower compared to the CalB strain, most probably due to the
392 accumulation of toxic methanol catabolism byproducts (i.e., formate) as previously reported
393 (Guo *et al.*, 2021). For both strains, the specific CalB lipase activity increased similarly over
394 time to reach values after 30 h of 113.6 and 113.3 U mgDCW⁻¹ for the CalB and the CalB-*fdh1Δ*
395 strains, respectively (Fig 5.D). On sorbitol, both strains exhibited similar lower biomass values
396 as compared to the glycerol medium. This could be lined with the lower uptake rate for sorbitol
397 compared to glycerol (0.02 g gDCW⁻¹ h⁻¹ and 0.9 g gDCW⁻¹ h⁻¹, respectively; data not shown).
398 Most importantly, the maximal specific lipase activity was remarkably higher for the FDH
399 disrupted strain (CalB-*fdh1Δ*) compared to the non-disrupted one (i.e. 130-fold). The specific
400 lipase CalB activity for the CalB-*fdh1Δ* strain was in the same range on sorbitol and sorbitol-
401 methanol medium (136 U mgDCW⁻¹ and 113.3 U mgDCW⁻¹, respectively). However, it was
402 reached 2.4 times faster on sorbitol medium (i.e. after 15h and 36 h, respectively, Fig 5F).



403

404 Figure 5. Biomass and specific lipase activity during growth of strains RIY 308 (pAOX1- α MF-
405 CalB, strain CalB, green squares) and RIY561 (fdh1 Δ -pAOX1- α MF-CalB, strain CalB- fdh1 Δ , -
406 blue triangles) in the presence of glycerol (YNBG, panels A and B), methanol-sorbitol (YNBMS,
407 panels C and D) and sorbitol (YNBS, panels E and F). Data are mean and standard deviation
408 from cultures were performed in triplicate in shake flasks in triplicate. Lipase assays were
409 performed in triplicates.

410

411

412 Conclusion

413 Herein, we have demonstrated that formate from the THF-C1 metabolism induces the pAOX1
414 promoter in an *fdh1 Δ* strain grown under derepressed culture conditions. This is particularly
415 interesting for recombinant protein production processes, as adding inducers such as
416 methanol or formate is no longer required to trigger rProt synthesis. By growing the cells in a
417 mixture of glycerol and sorbitol, rProt synthesis is initiated upon glycerol depletion in the

418 medium. This autoinduced system paves the way for further development of methanol-free
419 processes for rProt synthesis in *P. pastoris*.

420

421 **DATA AVAILABILITY**

422 Data are available upon request to the corresponding author

423

424 **FUNDING INFORMATION**

425 This research was funded by Becas Doctorado Nacional grant number 21211138-Agencia
426 Nacional de Investigación y Desarrollo (ANID), Chile; Doctoral Internship Scholarship (PUCV,
427 Chile); Research Stay Scholarship N° 018/2022 (Dirección de Postgrado y Programas,UTFSM,
428 Chile); Wallonie-Bruxelles International through the Cooperation bilateral Belgique-Chili
429 project SUB/2019/435787 (RIO4) and SUB/2023/591923/MOD (RIO6), FONDECYT Regular
430 (project number 1191196), University of Liege, Terra Teaching and Research Center.

431

432 **CONFLICT OF INTEREST STATEMENT**

433 The authors declare no competing interests.

434

435 **AUTHOR CONTRIBUTIONS**

436 **Cristina Bustos:** Conceptualization; data curation; formal analysis; investigation; methodology;
437 validation; visualization; writing – original draft; writing-review and editing. **Patrick Fickers:**
438 Conceptualization; formal analysis; investigation; methodology validation; validation;
439 visualization; funding acquisition; resources; supervision; writing – original draft; writing -
440 review and editing. **Julio Berrios:** Conceptualization; funding acquisition; supervision; writing-
441 review.

442

443 **ACKNOWLEDGEMENTS**

444 The authors thank Prof. Gasser from CD Laboratory of growth-decoupled protein production
445 in yeast, Department of Biotechnology, University of Natural Resources and Life Sciences for
446 providing pKTAC-Cre vector. A. Anckaert, M. Delvenne, Vandenbroucke, V., S. Steels and R.
447 Thomas are acknowledged for their technical help and fruitful discussion.

448

449 **BIBLIOGRAPHY**

- 450 Barone, G.D., Emmerstorfer-Augustin, A., Biundo, A., Pisano, I., Coccetti, P., Mapelli, V., and
451 Camattari, A. (2023) Industrial Production of Proteins with *Pichia pastoris* –
452 *Komagataella phaffii*. *Biomolecules* **13**: 441.
- 453 Berrios, J., Flores, M.O., Díaz-Barrera, A., Altamirano, C., Martínez, I., and Cabrera, Z. (2017) A
454 comparative study of glycerol and sorbitol as co-substrates in methanol-induced
455 cultures of *Pichia pastoris*: temperature effect and scale-up simulation. *J Ind Microbiol*
456 *Biotechnol* **44**: 407–411.
- 457 Berrios, J., Theron, C.W., Steels, S., Ponce, B., Velastegui, E., Bustos, C., et al. (2022) Role of
458 Dissimilative Pathway of *Komagataella phaffii* (*Pichia pastoris*): Formaldehyde Toxicity
459 and Energy Metabolism. *Microorganisms* **2022, Vol 10, Page 1466** **10**: 1466.
- 460 Bustos, C., Quezada, J., Veas, R., Altamirano, C., Braun-Galleani, S., Fickers, P., and Berrios, J.
461 (2022) Advances in Cell Engineering of the *Komagataella phaffii* Platform for
462 Recombinant Protein Production. *Metabolites* **12**: 346.

- 463 Carly, F., Niu, H., Delvigne, F., and Fickers, P. (2016) Influence of methanol/sorbitol co-feeding
464 rate on pAOX1 induction in a *Pichia pastoris* Mut+ strain in bioreactor with limited
465 oxygen transfer rate. *J Ind Microbiol Biotechnol* **43**: 517–523.
- 466 Collins, T.J. (2007) ImageJ for microscopy. *Biotechniques* **43**: 25–30.
- 467 Cotton, C.A., Claassens, N.J., Benito-Vaquerizo, S., and Bar-Even, A. (2020) Renewable
468 methanol and formate as microbial feedstocks. *Curr Opin Biotechnol* **62**: 168–180.
- 469 Ergün, B.G., Berrios, J., Binay, B., and Fickers, P. (2021) Recombinant protein production in
470 *Pichia pastoris*: from transcriptionally redesigned strains to bioprocess optimization and
471 metabolic modelling. *FEMS Yeast Res* **21**: foab057.
- 472 Feng, A., Zhou, J., Mao, H., Zhou, H., and Zhang, J. (2022) Heterologous protein expression
473 enhancement of *Komagataella phaffii* by ammonium formate induction based on
474 transcriptomic analysis. *Biochem Eng J* **185**: 108503.
- 475 Fickers, P., Nicaud, J.M., Destain, J., and Thonart, P. (2003) Overproduction of lipase by
476 *Yarrowia lipolytica* mutants. *Appl Microbiol Biotechnol* **63** : 136–142.
- 477 Guo, F., Dai, Z., Peng, W., Zhang, S., Zhou, J., Ma, J., et al. (2021) Metabolic engineering of
478 *Pichia pastoris* for malic acid production from methanol. *Biotechnol Bioeng* **118**: 357–
479 371.
- 480 Hartner, F.S. and Glieder, A. (2006) Regulation of methanol utilisation pathway genes in
481 yeasts. *Microb Cell Fact* **5**: 39.
- 482 Jayachandran, C., Palanisamy Athiyaman, B., and Sankaranarayanan, M. (2017) Formate co-
483 feeding improved *Candida antarctica* Lipase B activity in *Pichia pastoris*. *Res J Biotechnol*
484 **12**: 29–36.
- 485 Jhong, H.R.M., Ma, S., and Kenis, P.J. (2013) Electrochemical conversion of CO₂ to useful
486 chemicals: current status, remaining challenges, and future opportunities. *Curr Opin*
487 *Chem Eng* **2**: 191–199.
- 488 Kastanos, E.K., Woldman, Y.Y., and Appling, D.R. (1997) Role of mitochondrial and cytoplasmic
489 serine hydroxymethyltransferase isozymes in de Novo purine synthesis in
490 *Saccharomyces cerevisiae*. *Biochemistry* **36**: 14956–14964.
- 491 Krainer, F.W., Dietzsch, C., Hajek, T., Herwig, C., Spadiut, O., and Glieder, A. (2012)
492 Recombinant protein expression in *Pichia pastoris* strains with an engineered methanol
493 utilization pathway. *Microb Cell Fact* **11**: 22.
- 494 Lin-Cereghino, J., Wong, W.W., Xiong, S., Giang, W., Luong, L.T., Vu, J., et al. (2005) Condensed
495 protocol for competent cell preparation and transformation of the methylotrophic yeast
496 *Pichia pastoris*. *Biotechniques* **38**: 44–48.
- 497 Liu, B., Li, H., Zhou, H., and Zhang, J. (2022) Enhancing xylanase expression by *Komagataella*
498 *phaffii* by formate as carbon source and inducer. *Appl Microbiol Biotechnol* **106**: 7819–
499 7829.
- 500 Liu, B., Zhao, Y., Zhou, H., and Zhang, J. (2022) Enhancing xylanase expression of
501 *Komagataella phaffii* induced by formate through Mit1 co-expression. *Bioprocess*
502 *Biosyst Eng* **45**: 1515–1525.
- 503 Niu, H., Jost, L., Pirlot, N., Sassi, H., Daukandt, M., Rodriguez, C., and Fickers, P. (2013) A
504 quantitative study of methanol/sorbitol co-feeding process of a *Pichia pastoris*
505 Mut+/pAOX1-lacZ strain. *Microb Cell Fact* **12**: 33.
- 506 Piper, M.D., Hong, S.P., Ball, G.E., and Dawes, I.W. (2000) Regulation of the balance of one-
507 carbon metabolism in *Saccharomyces cerevisiae*. *Journal of Biological Chemistry* **275**:
508 30987–30995.

- 509 Prielhofer, R., Barrero, J.J., Steuer, S., Gassler, T., Zahrl, R., Baumann, K., et al. (2017)
510 GoldenPiCS: a Golden Gate-derived modular cloning system for applied synthetic
511 biology in the yeast *Pichia pastoris*. *BMC Syst Biol* **11**: 123.
- 512 Sakai, Y., Nakagawa, T., Shimase, M., and Kato, N. (1998) Regulation and physiological role of
513 the DAS1 gene, encoding dihydroxyacetone synthase, in the methylotrophic yeast
514 *Candida boidinii*. *J Bacteriol* **180**: 5885–5890.
- 515 Sambrook, J. and Russell, D.W. (2001) Molecular cloning: a laboratory manual, 3rd Edition.
516 New York: Cold Spring Harbor Laboratory Press.
- 517 Sassi, H., Delvigne, F., Kar, T., Nicaud, J.M., Coq, A.M.C. Le, Steels, S., and Fickers, P. (2016)
518 Deciphering how LIP2 and POX2 promoters can optimally regulate recombinant protein
519 production in the yeast *Yarrowia lipolytica*. *Microb Cell Fact* **15**: 159.
- 520 Schneider, C.A., Rasband, W.S., and Eliceiri, K.W. (2012) NIH Image to ImageJ: 25 years of
521 image analysis. *Nature Methods* **2012** 9:7 **9**: 671–675.
- 522 Sibirny, A.A., Ubiyvovk, V.M., Gonchar, M. V., Titorenko, V.I., Voronovsky, A.Y., Kapultsevich,
523 Y.G., and Bliznik, K.M. (1990) Reactions of direct formaldehyde oxidation to CO₂ are
524 non-essential for energy supply of yeast methylotrophic growth. *Arch Microbiol* **154**:
525 566–575.
- 526 Singh, A. and Narang, A. (2020) The Mut⁺ strain of *Komagataella phaffii* (*Pichia pastoris*)
527 expresses PAOX1 5 and 10 times faster than Mut^s and Mut⁻ strains: evidence that
528 formaldehyde or/and formate are true inducers of PAOX1. *Appl Microbiol Biotechnol*
529 **104**: 7801–7814.
- 530 Tyurin, O. V. and Kozlov, D.G. (2015) Deletion of the FLD gene in methylotrophic yeasts
531 *Komagataella phaffii* and *Komagataella kurtzmanii* results in enhanced induction of the
532 AOX1 promoter in response to either methanol or formate. *Microbiology (Russian*
533 *Federation)* **84**: 408–411.
- 534 Velastegui, E., Theron, C., Berrios, J., and Fickers, P. (2019) Downregulation by organic
535 nitrogen of AOX1 promoter used for controlled expression of foreign genes in the yeast
536 *Pichia pastoris*. *Yeast* **36**: 297–304.
- 537